INTERNATIONAL ATOMIC ENERGY AGENCY
UNITED NATIONS EDUCATIONAL, SCIENTIFIC AND CULTURAL ORGANIZATION

INTERNATIONAL CENTRE FOR THEORETICAL PHYSICS
34100 TRIESTE (ITALY) - P.O.B. 586 - MIRAMARE - STRADA COSTIERA 11 - TELEPHONES: 224281/9/2/4/5/6
CABLE: CENTRATOM - TELEX 460392 - I

H4.SMR/164 - 13

WORKSHOP ON CLOUD PHYSICS AND CLIMATE

23 November - 20 December 1985

ATMOSPHERIC CLOUD PHYSICS MEASUREMENTS -II

(Extra lecture notes)

C. SAUNDERS

University of Manchester, U.K.

Calibrated Thermometer

Mercury or Alcohol

Accuracy 0.1°c

Thermocouple

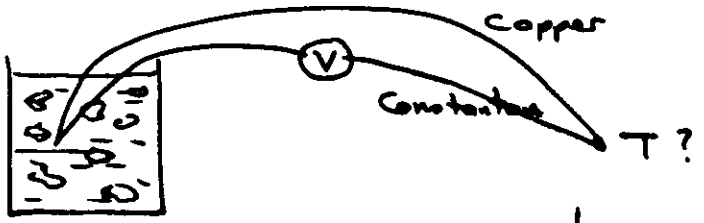

Constant Temperature
Both . Ice/water at 0°c.

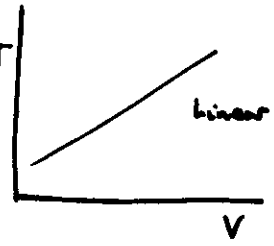

Accuracy 0.01°c

Thermistor

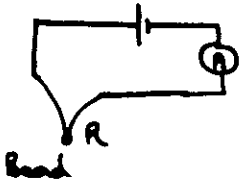

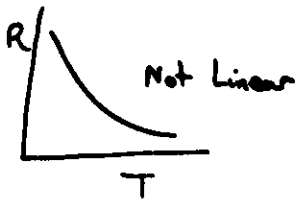

Accuracy 0.1°c

Platinum Resistance Thermometer

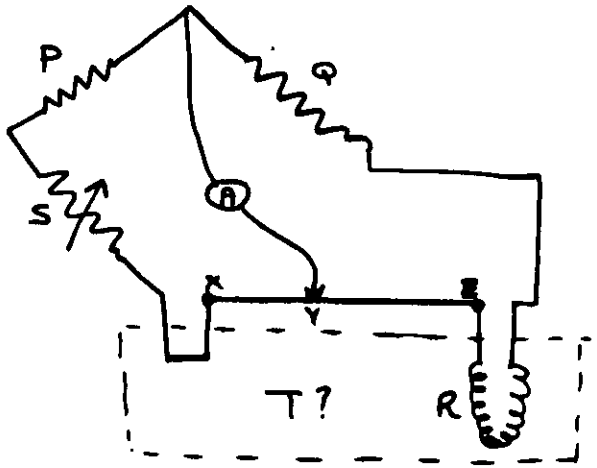

$$\frac{P}{Q} = 1 = \frac{S + (r\,XY)}{R + (r\,YZ)} \qquad \text{For } A = 0$$

r = resistance / length of wire XZ.

Manufacturers give R/T data in form of polynomial.

Linearising Circuit

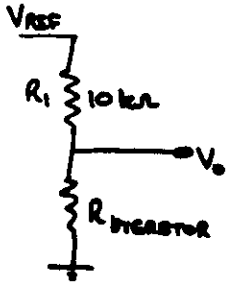

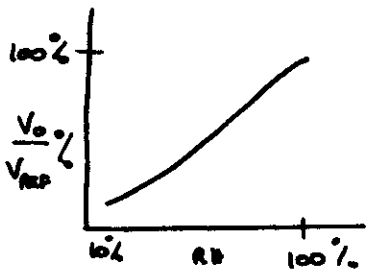

5) Direct Capacitance Method.

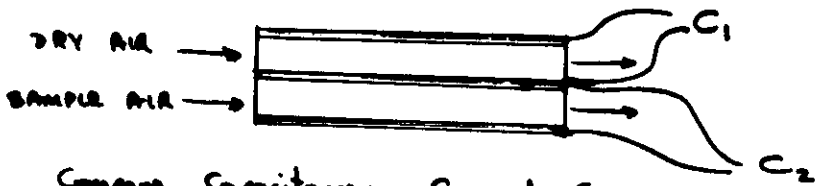

Compare Capacitances C_1 and C_2

$(\varepsilon-1)$ for dry air = 6×10^{-4}

$(\varepsilon-1)$ for H_2O vapour = $1.6 \times 10^{-4} \rho$

$\rho \equiv g\ m^{-3}$.

Dew Point (Frost Point)

Cambridge hygrometer

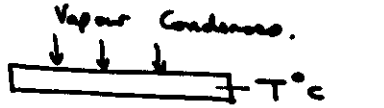

Liquid Water Content

1) Psychrometric Method. See Wishart pp 3 and 22

2) Rotating Impactor. Need Collision Efficiencies.

Humidity Measurements

1) Wet and Dry bulb.
(Sling psychrometer)

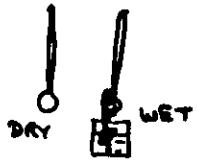

2) Lyman α Absorption. 121nm (Kyle)
(Fast Response, $2000/sensor, optics prone to NaCl damage.)

3) Capacitance.

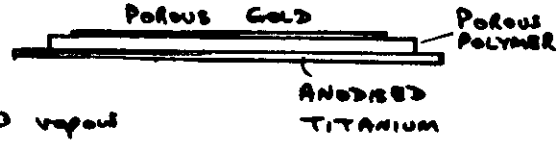

Polymer absorbs H_2O vapour
known changes. C = 500pf ± 1pf / % RH change
Linear response. (2 seconds) Contaminant Sensitive
Cat $50 from Lee Integer, Vaisala.

4) Carbon Hygristors

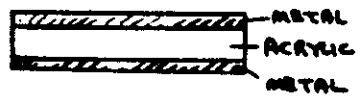

Acrylic/carbon absorbs H_2O which changes R.
Response Time 0.2s.

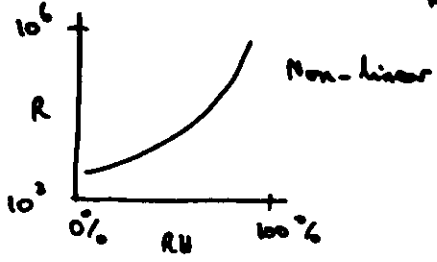

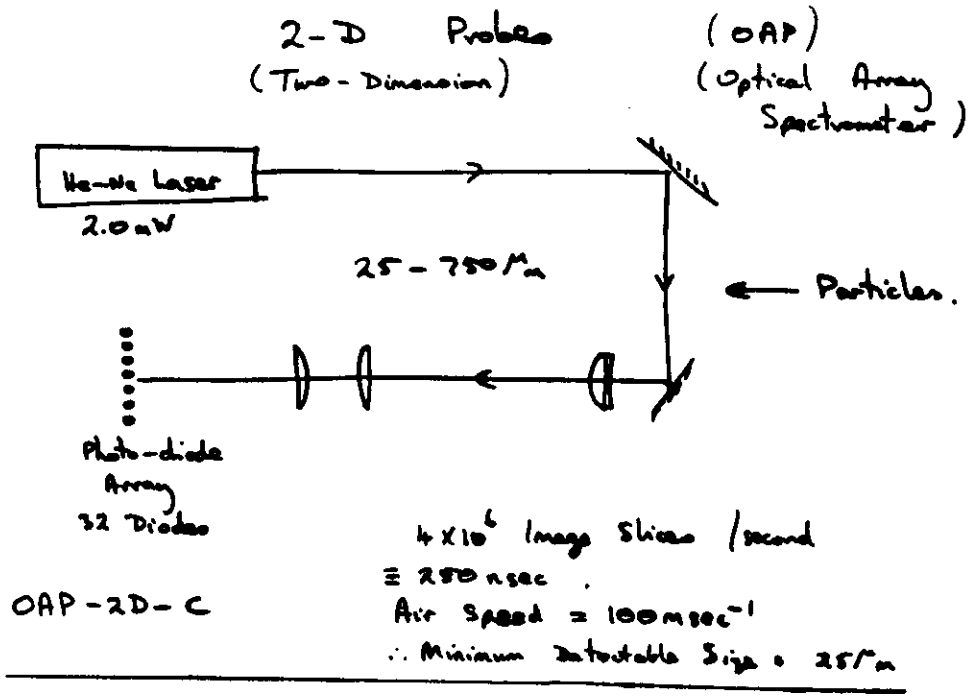

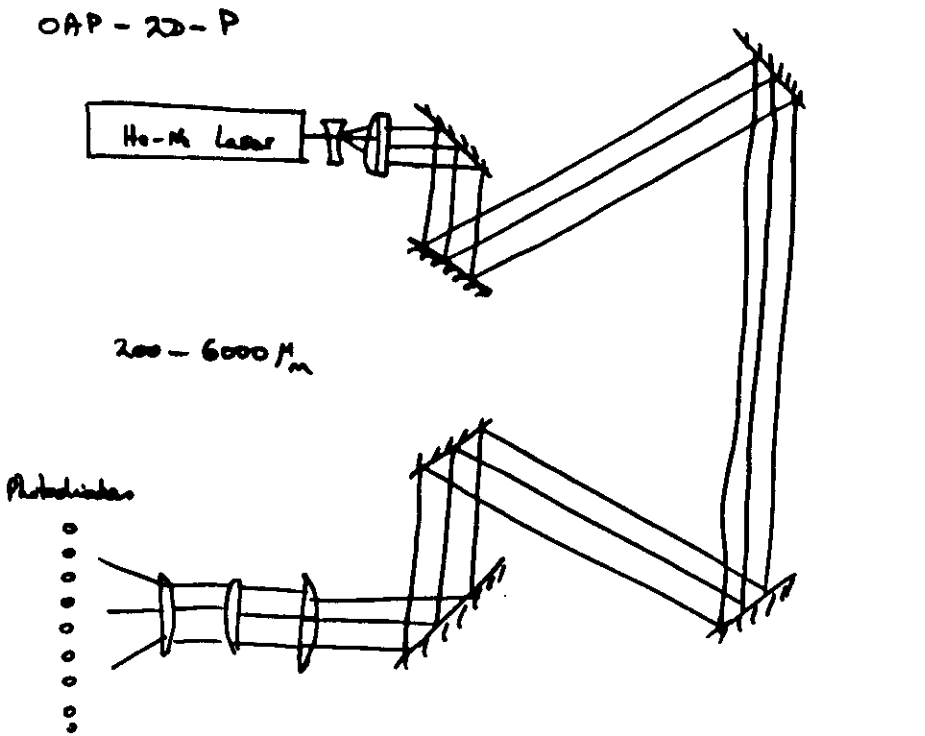

radar pulses. Studies of hydrometeors using airborne imaging devices correlated with one or more radars observing the same region of cloud or precipitation as the aircraft will lead to further understanding of storms.

● Are automatic particle-counting and sizing instruments giving an accurate representation of the cloud being observed? By giving the scientist a "look" at the cloud, imaging devices serve as a check on the integrity of data coming from other counting and sizing instruments. Data from electronic and electro-optical devices may be influenced by electronic noise, icing, or collection efficiency problems that might otherwise go undetected if the data look reasonable. Automatic sizing instruments give the size of the projected image; the measured size depends on orientation of the particles. This orientation can often be determined with imaging instruments. The accuracy and interpretation of impressions or replicas can also be checked by comparison with images obtained using imaging devices.

We will describe three imaging devices currently in use—the two-dimensional optical array spectrometer probe of Particle Measuring Systems (PMS), Boulder, Colorado; the NCAR particle camera; and the airborne holography system of Science Applications, Inc., El Segundo, California.

The Optical Array Spectrometer Probe

The PMS two-dimensional array spectrometer probe, developed under the direction of Robert Knollenberg (of PMS), is a unique variation of the optical array particle-sizing probe described in the article by A. Heymsfield in this issue. In the sizing probe, the particles pass through a parallel light beam from a continuously radiating laser and a shadow is cast on a linear array of light sensors (photodiodes) located in the beam. The size of each particle is determined by electronically counting the number of sensors with light extinguished below a 50% intensity threshold by the shadow. In the two-dimensional probe, the entire array of sensors is sampled at a "slice" rate proportional to the true airspeed. By use of a high-speed, front-end data storage register, each sensor can transmit up to 1,024 bits of shadow information for each particle. A series of "image slices" is recorded across the shadow to develop a true two-dimensional image.

Figure 1 illustrates the data format for a dendritic ice crystal. All together in the basic probe there are 32 sensors in the linear array, each imaging a portion of the light beam 25 μm in diameter. Because of the shadow cast by the particle, the light level falls to the threshold of detectability (50%

Fig. 1 Star-shaped dendritic ice particle passing across optical array of PMS two-dimensional probe is imaged as a matrix of zeros and ones, depending on absence or presence of light (at 50% extinction) on the optical sensors during each slice.

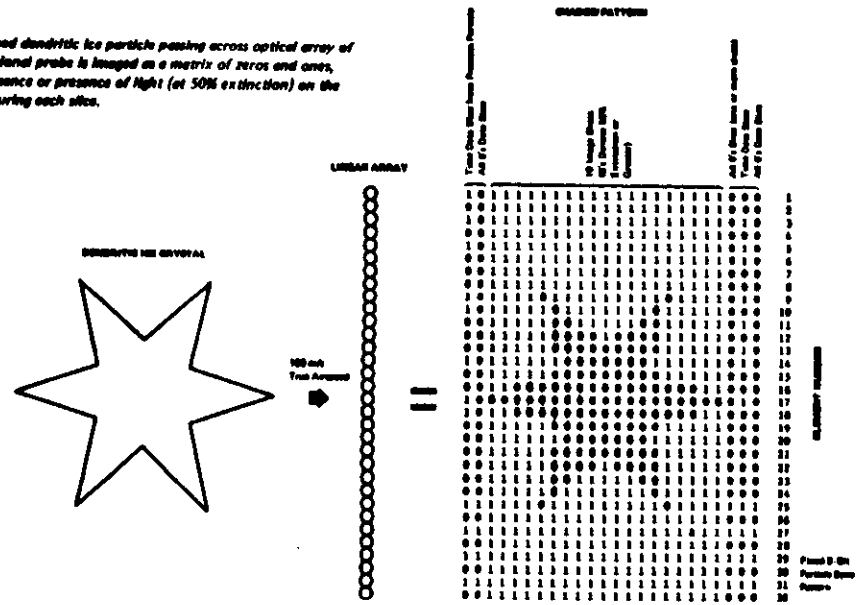

3

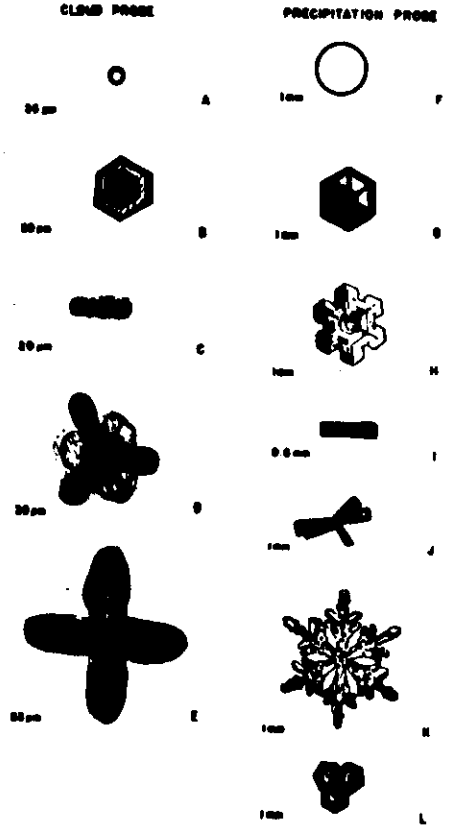

Fig. 4 Parts A - E are tracings of ice crystal microphotographs for sizes smaller than 100 μm as they would appear if viewed from above or focused on the optical array of the probe. Parts F - L are ice crystals larger than 300 μm as they would be focused on the optical array of the precipitation probe.

Parts B-E of Fig. 4 show tracings of ice particles smaller than 100 μm in length, which one would expect to be sized by the cloud probe. The plate ice crystal (B) is generally oriented with its long axis horizontally aligned to the array, and its cross section is therefore read as nearly spherical. The depth of field will be the same as that for a sphere of equivalent diameter, it will be sized properly, and the calculated concentration will be correct. But consider the column in part C. Its long axis will be horizontal in the atmosphere, but its orientation will be random when it passes through the linear optical

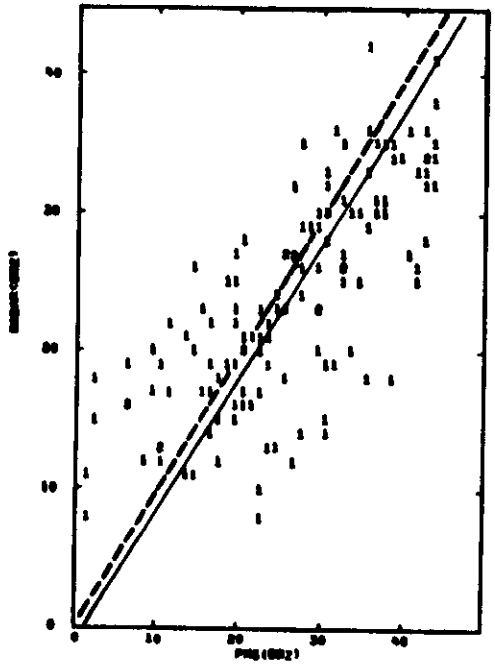

Fig. 5 Radar reflectivity factor measured by NSSL radar (dBZ = 10 log Z) and calculated from PMS precipitation probe in nearly the same region of the cloud. Each 1 point is a 1 km average, and a 2 point indicates two 1 km points on top of each other. The dashed line is at 45°, and the solid line is a least-squares curve through the data points.

PROBE / RADAR Comparison
in rain.

array. Therefore, it will be read at values ranging from its full length (20 μm) to its width (6 μm) when passing through the array. A 100 μm column with a similar length-to-width ratio may be sized anywhere from 100 μm to about 30 μm. The distributions can be "transformed" on the basis of this random columnar crystal orientation (Heymsfield and Knollenberg, 1972) if all the particles are columnar.

Other problems may be associated with measuring the columnar particle in part C. Assume that it passes through the array at its full length. Even if in perfect focus on the array, its cross-sectional area per channel will be $6 \times 20 = 120\ \mu m^2$, compared to the channel cross-sectional area of $20 \times 20 = 400\ \mu m^2$. Therefore, the reduction of light intensity will be 120/400 = 30%, not enough to trigger the flip-flop switch or to register a count as a particle. In addition, the

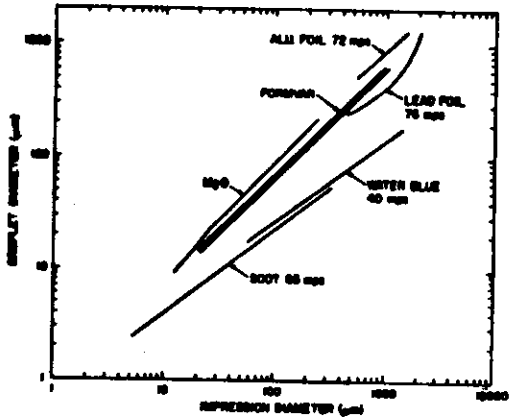

Fig. 1 Relation between droplet diameter and impression diameter for various sampling media.

Fig. 2 Drop impressions in soot layer. (Photo courtesy of J. Dye, NCAR.)

Slide Impactors

• *Oil-Coated Slides.* One of the earliest measurements of cloud droplet sizes was made by Fuchs and Petrjanoff (1937). A clean glass slide coated with a mixture of light mineral oil and petroleum jelly was used to capture cloud droplets and keep them submerged until they had been photographically recorded. The method was improved and used in an aircraft by Mazur (1943), who saturated the mineral oil with distilled water to prevent the droplets from diffusing into the oil.

Slides coated with castor oil were used in the first extensive set of measurements of droplet sizes in cumuliform clouds by Weickman and Aufm Kampe (1953). With this method it was possible to collect droplets as large as 200 μm in diameter with no apparent shattering if the impact velocity was less than 100 m/s.

A large amount of droplet data was obtained by an automated sampler designed by Brown and Willett (1955). In their sampler three slides coated with silicone oil moved in rapid succession through an airstream and were photographed under a microscope in a cold cabin. The results for mean droplet distributions in trade-wind and summertime U.S. continental cumuli were reported by Braham, Battan, and Byers (1957) and by Battan and Reitan (1957).

These methods gave us the first details of the droplet spectrum at different geographical locations. A disadvantage of using them is that the sample must be recorded immediately, a procedure which is difficult in turbulent air. It is also necessary to know the exact time that elapsed between sampling and recording in order to apply diffusion corrections.

• *Magnesium Oxide Method.* Another widely used method involves coating a clean glass slide with a thin film of magnesium oxide. Droplets impinging on the film leave round holes which are proportional to their size.

This technique was developed and calibrated by May (1950) for drop diameters between 10 and 240 μm. For droplets larger than 20 μm in diameter, the ratio of droplet diameter to impression diameter was found to be 0.86; it remains constant with droplet size. Data reduction requires the investigator to examine the slide surfaces by microscope with a strong transmitted light and record the images photographically. This method is not affected by drop diffusion and droplets cannot coalesce, so the samples can be preserved. One disadvantage is that this layer is rather fragile in texture and can break off because of buffeting by the airstream. Another is that drops below 8 μm in diameter cannot be sized with certainty because the texture and grain size of the magnesium oxide interfere. Squires and Gillespie (1952) used this technique in a gun-type sampler which could be reloaded in about 50 s during flights. They exposed ten rods 3 mm wide (yielding a high collection

The foil impactors provided our first drop-size distributions for precipitation-sized particles (>250 μm in diameter) in natural clouds. Yet there are still problems with these devices. One is that it is difficult to obtain a representative sample of large drops if they occur in low concentrations. Increasing the sampling volume yields an overexposure of the smaller drops, resulting in overlapping of the imprints. Moreover, during icing conditions instrument reliability depends on how successfully deicing elements were employed. It is not always possible to make a clear distinction between liquid and solid hydrometeors from impressions obtained in a mixed-phase cloud. Calibration of imprints is not available for solid particles. Under all conditions, data handling and analysis are tedious and subjective.

Replicator Devices

Replicator devices have been widely used in cloud physics studies. They are mechanized sampling devices using the well known Formvar technique to capture and permanently encapsulate cloud particles (see MacCready and Todd, 1964; Spyers-Duran and Braham, 1967; Spyers-Duran, 1972a). They utilize a Mylar tape (usually a 16 mm polyester leader) which is coated with a solution of Formvar plastic and chloroform. (For airborne use, chloroform is preferred since it is nonflammable.) The continuously moving ribbon of Formvar is exposed in a cloud through a sampling slit several millimeters wide and then carried into a drying compartment where the plastic sets quickly. There, the encapsulated particles evaporate, leaving behind permanent replicas which can be sized and counted after suitable magnification. Since it is possible to obtain a continuous record through a cloud, the replicas can provide small-scale resolution of changes in cloud microstructure. Recently developed devices have the capability of viewing the replicas shortly after exposure so that tape speed and Formvar thickness can be adjusted in flight, as reported by Christensen, Keller, and Hallett (1974). Another major advantage of this method is that simultaneous recording of cloud droplets and ice crystals is possible (see Fig. 5).

Basically these devices are simple; however, they require a great deal of design compromise. In designs in which coatings

(a)

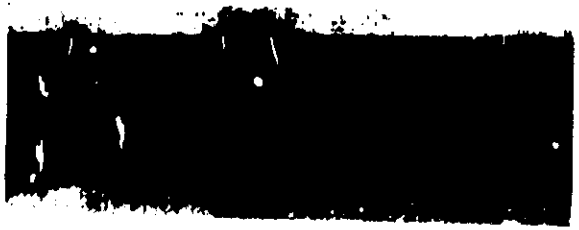

(b)

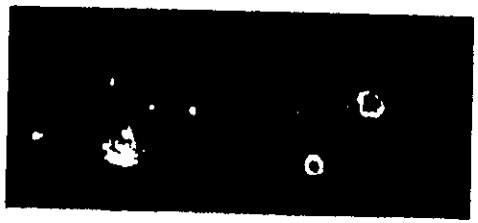

Fig. 4 Impressions of precipitation-sized particles in a lead foil exposed on the University of Chicago Lodestar aircraft (a), and in aluminum foil exposed on the South Dakota School of Mines and Technology T - 28 aircraft (b). Smallest diameter is 250 μm. (Sample a, courtesy of E. Brown, NCAR; sample b, courtesy of C. Knight, NCAR.)

Fig. 5 Replicas of supercooled droplets (A), a snow pellet (B), and ice crystal columns (C).

RADKE - TURNER ICE CRYSTAL PROBE

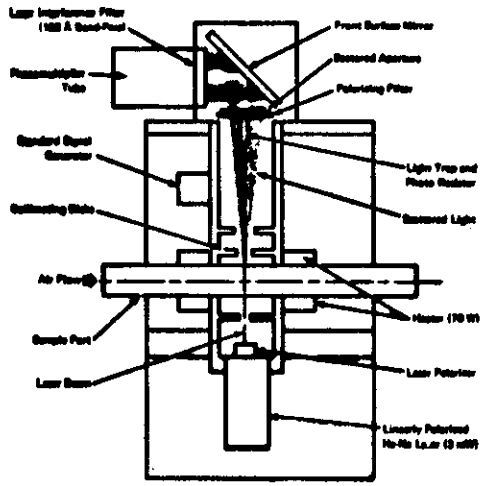

Fig. 1 Schematic representation of the University of Washington's automatic optical ice particle counter.

system so that linearly polarized infrared light is incident on particles passing through the sample pipe. The light sensor (a solid-state device) detects the infrared light that is scattered at an angle of 90° (actually a cone of light around a scattering angle of 90°) after the light passes through an optical system containing a polarizing filter set for maximum extinction.

It can be seen from the description of the two instruments that the UW-IPC detects forward-scattered light while the Mee-IPC detects light scattered at an angle of 90°. As we will see below, this difference becomes important in discussing the mechanisms for the detection of ice particles in the two systems.

Mechanisms for Ice Detection

There are three possible mechanisms for the detection of particles in the two devices described above (see Turner and Radke, 1973, for a more detailed discussion):

- The rotation of the plane of polarization of the light beam, produced by the birefringent property of ice, as it passes through the ice particles
- The detection of specularly reflected light from the external faces of ice crystals
- The detection of light scattered at a preferred angle by the ice particles.

Owing to the birefringent (or double refracting) property of ice, linearly polarized light that is transmitted through ice will generally, be rotated in such a way that although the light

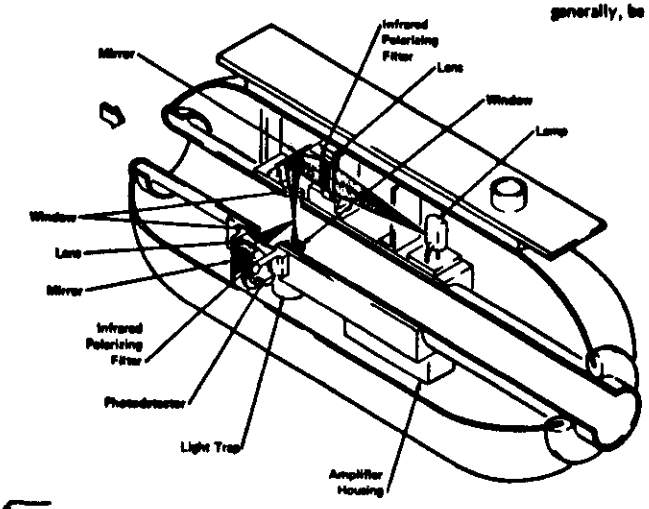

Fig. 2 Schematic diagram of the Mee Industries automatic optical ice particle counter. The pod is 45.7 cm (18 in.) long and 17.8 cm (7 in.) in diameter. The cylindrical opening in its center is 5.1 cm (2 in.) in diameter.

STATIC DIFFUSION CHAMBER FOR CCN

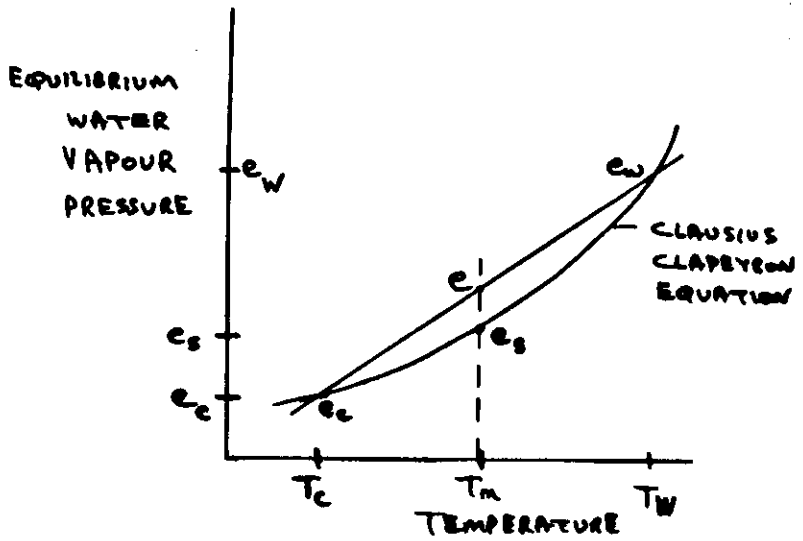

Saturation Ratio, $s_w = \left(\frac{e_w - e_a}{2} + e_a\right) \Big/ e_s$

$s_w = (e_w + e_c) / 2e_s$

Supersaturation % $= (s_w - 1) \times 100$

$$S_w = \left(\frac{(e_w + e_c)}{2e_s} - 1\right) \times 100 \quad \%$$

Camera views drops.

Ice Nuclei Detection.

Deposition Nuclei : Filters + Static Diffusion Chamber or Continuous Flow Chamber below Water Saturation.

Condensation Freezing Nuclei : Continuous Flow chamber above water saturation.

Contact Nuclei : Drop Freezing (Vali)

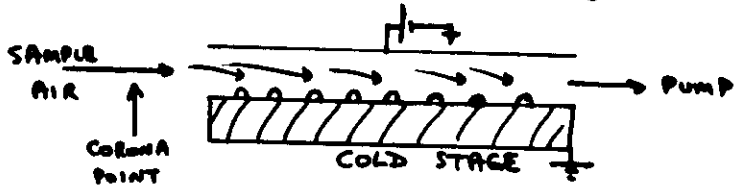

Charged nuclei are deflected in field onto supercooled (pure) water drops.

Immersion Nuclei Sample Drop Freezing (Vali)

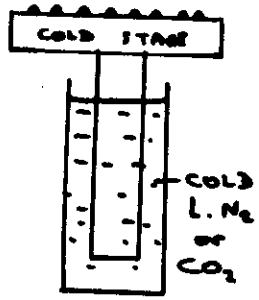

Cool drops containing the nuclei and watch for them to freeze. Note the number freezing at each temperature.

Contact Nuclei Spray Technique

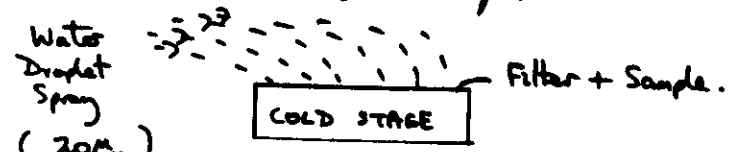

DIFFUSION BATTERY

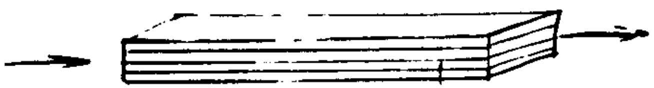

Many plates. Small particles diffuse to the plates and are captured. Only the large particles pass through.

Cascade Impactor

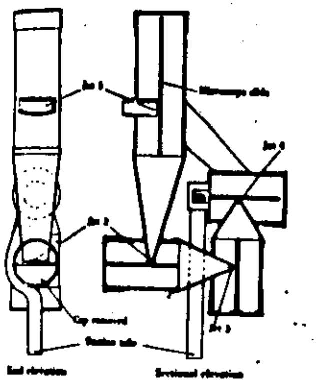

Fig. 1. Diagram of cascade impactor

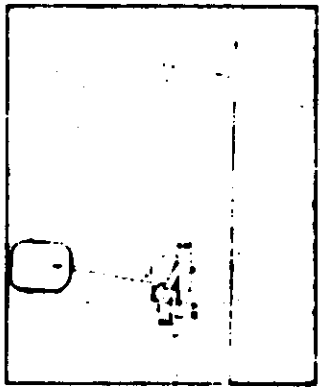

Aircraft Measurements

a) Vertical Wind. ~ 1 second (100m) resolution.

i) Cheap method: Slow down and let the plane "follow" the air vertical velocity. Find the vertical velocity from the altimeter rate of change.

ii) Accurate method: $W_{ag} = W_{ap} + W_{pg}$

W_{ap} = Air vertical velocity with respect to plane.
W_{pg} = Plane " " " " " ground.
W_{ag} = Air " " " " " " .

$$W_{ag} = TAS \sin(\theta - \alpha) + \int a_z \, dt$$

↑ True Air Speed ↑ Vertical Acceleration.

$$TAS = IAS \left(\frac{0.1309\,(°K)}{\text{Pressure Alt in " of Hg}} \right)$$

IAS = Indicated Air Speed. (from Pitot Tube)

Pitch, Θ, Vertically stabilised accelerometer. (VSA)

α, Vane on nose boom, or side of aircraft.

W_{pg}, from the VSA.

b) Horizontal Wind. Doppler System + Yaw Vane.

$$V_{ag} = V_{ap} + V_{pg}$$

Wind = Air relative to ground; V_{ap}: Air relative to plane; V_{pg}: plane relative to ground

Doppler radar → V_{pg}. TAS + Yaw Vane Angle → V_{ap}.

Objective To increase ice particle concentration.

Aims 1) Ice clouds are more efficient than water clouds at producing precipitation. [Increased Rainfall]

2) To reduce damage to crops from hail. [Hail Suppression.]

---

1) To Increase Precipitation:

a) Cloud physics study of clouds — is there water available in the cloud? Can this water be frozen by seeding? Will the precipitation fall where you want it?

Increase buoyancy! Dynamic Seeding eg Florida.

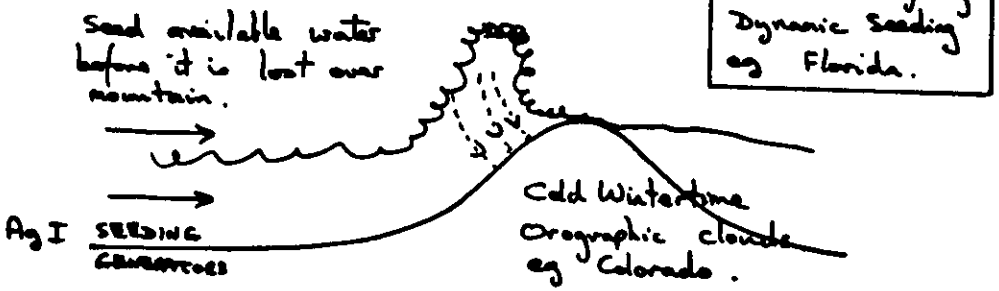

2) To Reduce Hail:

Methods 1) Total Glaciation — Ice Crystals below awng. > 10gm AgI/min/km². Too Expensive.

2) Beneficial Competition. Many small particles compete for available water — so insufficient water for large hail to grow.

Works best for storms with warm cloud bases — frozen-drop embryos are efficient hail producers — so artificially seeded frozen-drop embryos give competition.

Storms with cold bases have graupel embryos which start on small crystals higher up — competition seems inadequate. [eg Colorado]

Cloud Seeding (2)

Agents AgI — NH_4I — Acetone. (Better epitaxial fit than AgI.)

still active 90km downwind. (4hrs) No deactivation.

Cheaper is Titanium Oxide coated with AgI (20% coat)

Pyrotechnic Flares at cloud base — 400 Xtals/l after 4 mins. Aggregates in 13 mins. Traced by glider. 10^{11} particles / gm of AgI.

Burn a AgI — acetone mixture on the ground or on aircraft generators. (400gm/hr.)

Top seeding, −4° C, 16 — 20,000', into feeder towers. 50gm droppable pyrotechnic flares.

Traces To check whether seeding agent would get into the cloud at the right place.

eg Tag AgI with Titanium Dioxide. Detect on captured precipation with ion probe analysis.

Other Methods

Carbon black, 0.1 Mm particles — absorb solar energy.

Cool by releasing compressed air or gas.

Warm Rain — Hygroscopic seeding — NaCl — Langmuir chain reaction — drop breakup. Models show need for ≥ 10 ms⁻¹ updraught. No results yet.

Fog — Helicopter Downwash — mixing.
— Water jets to wash-out fog.